Carbohydrate Polymers 354 (2025) 123329

Contents lists available at ScienceDirect

Carbohydrate Polymers

journal homepage: www.elsevier.com/locate/carbpol

Gellan-based hydrogels and microgels: A rheological perspective

Silvia Franco [a,b,*], Leonardo Severini [a,b], Elena Buratti [c], Letizia Tavagnacco [a,b], Simona Sennato [a,b], Laura Micheli [d], Mauro Missori [a,b], Barbara Ruzicka [a,b], Claudia Mazzuca [d], Emanuela Zaccarelli [a,b,*], Roberta Angelini [a,b,*]

[a] Institute for Complex Systems, National Research Council, Sede Sapienza, Piazzale Aldo Moro, 5, Rome 00185, Italy
[b] Physics Department, Sapienza University of Rome, Piazzale Aldo Moro 5, Rome 00185, Italy
[c] Department of Chemical, Pharmaceutical and Agricultural Sciences, University of Ferrara, Via L. Borsari 46, Ferrara 44121, Italy
[d] Department of Chemical Science and Technologies, University of Rome Tor Vergata, Via Della Ricerca Scientifica 1, Roma 00133, Italy

ARTICLE INFO

Keywords:
Microgels
Hydrogels
Rheology
Gellan gum
Paper artwork cleaning
Monovalent and divalent cations

MSC:
0000
1111

ABSTRACT

Gellan gum-based systems have gained significant attention due to their versatility for multiple applications. In particular, they have shown a great potentiality in the field of cultural heritage, as efficient paper artwork cleaning agents in restoration processes. This efficacy is enhanced when gellan gum is assembled to form stable microgels, by controlling the gelation process under shear. Moreover, the use of methacrylated gellan gum provides additional functionality to the systems, that are also able to remove hydrophobic residues during the cleaning process. However, in order to optimize the manufacturing process, it is fundamental to obtain a thorough understanding of the rheological behaviour of the employed gellan gels in the optimal working conditions for paper cleaning. The present work aims to thoroughly characterize the rheological properties of low-acyl gellan gum, also during hydrogel and microgel formation, assessing the role of temperature (25–80 °C), gellan concentration (0.5–5 % for hydrogels and 0.1–0.5 % for microgels), methacrylation, presence of different cations (Na^+, Ca^{2+}) and salt concentration (0.25–5.0 mM for hydrogels and 100 mM for microgels), on the behaviour of viscosity and viscoelastic moduli. We find the notable result that gellan hydrogels and microgels exhibit a double yielding behaviour in the conditions where they are mostly efficient for art restoration. Furthermore, we identify the optimal rheological conditions of these gels for efficient artwork restoration, opening the possibility to extend their applications to different substrates and in other fields.

1. Introduction

Gellan gum (GG) is a polysaccharide derived from microbial fermentation of sugars by the bacterium Sphingomonas elodea and commonly employed in manufacturing sectors such as food, pharmaceutical, and cosmetic industries, due to its gelling, stabilizing, and thickening properties (Oh et al., 2008; Picone & Cunha, 2011; Sworn et al., 1995). Its repeating unit consists of a tetramer of one (1,3)-β-D-glucose, one (1,4)-β-D-glucose, one (1,3)-β-D-glucuronic acid, and one (1,4)-α-L-rhamnose (Sworn et al., 1995). The ability of GG to form stable physical gels, its compatibility with a wide range of ingredients, the versatility in modifying texture and consistency as well as its easiness in chemical modification have contributed to its widespread use in many fields. In particular, for food processing and production, it serves as a gelling agent, stabilizer, and thickener, enhancing the texture and stability of products like jams, jellies, and dairy alternatives (Banerjee & Bhattacharya, 2012; Morris et al., 2012; Saha & Bhattacharya, 2010). In pharmaceutics and biomedicine, GG is utilized for controlled drug delivery (D'Arrigo et al., 2014; Matricardi et al., 2009; Milivojevic et al., 2019), as a delivery system for superficial cutaneous administration (Musazzi et al., 2018), in tissue engineering (Gajbhiye et al., 2024; Oliveira et al., 2010), and as a bioink in 3D printing to create cell-laden constructs (Compaan et al., 2019). Its ability to form strong, clear gels makes it also valuable in cosmetic formulations for products such as lotions and creams (Nagpal et al., 2019). In addition, GG is used in the agricultural sector as fertilizer-release agents (Sabadini et al., 2015), for seed coating and as a component in plant tissue culture media.

Commercially, gellan gum is available in different forms. In its native form it contains two acyl moieties, L-glyceryl and acetyl groups, linked to the (1,3)-β-D-glucose residue. When the acyl groups are removed by

* Corresponding authors at: Institute for Complex Systems, National Research Council, Piazzale Aldo Moro, 5, Rome 00185, Italy.
E-mail addresses: silvia.franco@cnr.it (S. Franco), emanuela.zaccarelli@cnr.it (E. Zaccarelli), roberta.angelini@cnr.it (R. Angelini).

https://doi.org/10.1016/j.carbpol.2025.123329
Received 5 August 2024; Received in revised form 20 January 2025; Accepted 27 January 2025
Available online 30 January 2025

alkaline hydrolysis, two types of Gellan gum can be obtained: high-acyl GG, where the acyl groups are partially removed, and low-acyl (or deacylated) GG, where the acyl groups are completely removed. The acylation degree affects the rheological and mechanical properties of the resulting physical hydrogel: high-acyl GG leads to soft, elastic, and opaque hydrogels, while deacylation allows to obtain rigid and compact hydrogels, characterized by a high degree of viscoelasticity and a remarkable transparency (Chandrasekaran et al., 1988; García et al., 2011; Morris et al., 2012; Tang et al., 1997). Deacylated GG sol-gel transition is an exothermic process (Miyoshi et al., 1996) during which GG chains in aqueous dispersion once heated ($T \geq 90^{\circ}$), assume a random coil conformation; subsequently, in the cooling process, they undergo a transition from a disordered to a more ordered state, through the formation of single or double helices due to spontaneous self-assembly (coil-helix transition) (Diener et al., 2019; Diener et al., 2020; Miyoshi & Nishinari, 1999a). Upon further cooling, there is an association between the helical structures, leading to a sol-gel transition. As early as 1999, Miyoshi and Nishinari (Miyoshi & Nishinari, 1999b) investigated the viscosity behaviour of GG with temperature in the concentration range 1–5 % and demonstrated that GG undergoes a sol-gel transition upon cooling or through the addition of salts. In particular, they showed that an aqueous dispersion of gellan gum passes from a dilute polymer dispersion to a weak gel, which can be controlled by polymer concentration and temperature. This can happen even in the absence of salt, thanks to increased molecular entanglement and enhanced intermolecular interactions. However, the addition of salt facilitates gel formation, improving its stability and structure. In particular, divalent cations facilitate the formation of junction zones leading to the formation of more stable gels as compared to monovalent ones, due to their ability to interact with multiple binding sites on the gellan gum chain. This was confirmed by rheological measurements combined with differential scanning calorimetry (DSC) (Miyoshi & Nishinari, 1999b). For gellan gum solutions at low concentrations, the cooling and heating DSC curves were found to display a single exothermic or endothermic peak, which shifts to higher temperatures as the gellan gum concentration increases. Based on this pioneering investigations, Miyoshi and Nishinari proposed a phase diagram illustrating the three different physical states of gellan gum: coil conformation, helix conformation in liquid states and ordered structures leading to gels. Several other studies also reported that the rheological properties of GG are significantly influenced by various factors, including the concentration of polysaccharides, the working temperature and the charge and type of added cations (Miyoshi et al., 1996; Miyoshi & Nishinari, 1999b; Tang et al., 1997; Yang et al., 2024). However, beside the work of Miyoshi and Nishinari, rheological measurements on gellan gum are present in the literature only at relatively low GG concentration (up to 1%), in the presence or absence of salts (Caggioni et al., 2007; Nickerson et al., 2003; Paulsson et al., 1999). This is a critical lack of data because the new frontiers opened by various applications of this polysaccharide and the potentialities offered by the chemical modifications of its residues require a deep knowledge of the rheological properties of gellan gum gels at higher concentrations. To fill this gap, our study examines pure gellan hydrogels within a concentration range similar to that of ref. (Miyoshi & Nishinari, 1999b), extending the lower boundary to 0.5 wt%. More importantly, the evolution of viscoelastic moduli under shear strain and the plateau moduli have been extensively investigated varying concentration, temperature, and cation type (monovalent, divalent). In particular, one promising field of application of GG gels is given by paper artwork cleaning. In fact, in the last few years, GG hydrogels have emerged as efficient wet cleaning treatments for paper artworks (Khaksar-Baghan et al., 2024). Wet cleaning is a very delicate operation, and to be used for this purpose, hydrogels must fulfill several strict conditions from the mechanical point of view: i) they have to be easily handled, applied and removed on paper sheets to be cleaned without breaks and leaving residues; ii) they have to be able to stand quite significant pressures without breaking. This is because a weight is usually applied to the hydrogel to ensure a close contact between the gel and the artwork to be cleaned. Typically, for a round portion of a gel with 3 cm of radius, a weight of about 150 g may be used; this means that the pressure on the gel is about 520 Pa (Micheli et al., 2016). At the same time, they have to be soft enough, so that the solvent can effectively exert its cleaning action without wetting the sample too much and then be removed together with the gel itself. Therefore, a deep knowledge of the rheological properties of gels to be used for cleaning is of fundamental importance to avoid unwanted damages on artworks. In addition, we recently put forward the use of gellan gum and methacrylated gellan gum microgels as cleaning tools in the paper artwork restoration (Di Napoli et al., 2020; Severini et al., 2025), as they ensure a very fast cleaning with efficacy close to or higher than the corresponding GG hydrogels. Furthermore, we recently unveiled the molecular origin of the two-step aggregation of gellan gum by numerical simulations (Tavagnacco et al., 2023). We hypothesize that this two-step mechanism must have a clear rheological signature that we investigate in the present work. Moreover, we believe that the knowledge of the rheological behaviour of gellan gum-based hydrogels and microgels will be critical for optimizing their application in the cleaning of paper artwork. To this aim, we perform an extensive rheological characterization of GG hydrogels in the concentration range (0.5–5 %) in presence of different cations (Na^{+}, Ca^{2+}), by varying salt content (0.25–5.0 mM) and upon methacrylation. Moreover, we investigate in detail the viscoelastic properties of GG and GG methacrylated microgels in the concentration range (0.1–0.5 %) at fixed monovalent salt (100 mM), after discussing our newly established and reproducible preparation protocol. All discussed cases refer to the conditions in which we have already tested the ability of the hydrogels and microgels to efficiently clean paper artwork.

2. Materials and experimental methods

2.1. Materials

Low acyl gellan gum powder Kelcogel™, was from CP Kelco (KELCOGEL, San Diego, California, CAS: 71010–52-1; Lot: 9G6158A) with molecular weight 2–3·10^5 Daltons and dry substance content (DS content) 4–5%. The Chemical composition of deacetylated gellan gum is: neutral sugars Glc/Rha = 6/4 of 62, acetyl group 0%, uronic acid 13%, protein 17% and ash 8% (Prajapati et al., 2013). The absence of the acetyl groups, within gellan chains, was confirmed by the analysis of NMR data reported in Severini, et al. (Severini et al., 2023). Indeed, the peak at 2.16 ppm of the ^{1}H NMR spectrum assignable to the methyl proton of acetyl groups according to (Cai et al., 2024) is not visible. As demonstrated in the literature, using atomic absorption, low acyl gellan gum (KELCOGEL LA) contains the following average ionic composition: Na^{+}: 6330 ppm; K^{+}: 46800 ppm; Ca^{2+}: 3660 ppm; and Mg^{2+}: 1140 ppm (Sworn & Kasapis, 1998). Glycidyl methacrylate, sodium chloride, calcium acetate hydrate, sodium oxide were from Merk (Merk KGaA, Darmstadt, Germany). Reagents used in this work were of analytical grade and used without further purification. Ultrapure water (resistivity: $18.2 M\Omega/cm$ at 25 °C), obtained with Arium® pro Ultrapure water purification Systems, Sartorius Stedim, was used for the solution preparation. GG methacrylation occurred as reported previously (Severini et al., 2023).

2.2. Gellan gum methacrylate (GGMA) preparation

GGMA was prepared according to a procedure reported elsewhere (Severini et al., 2023). GG was dissolved in distilled water at a concentration of 1% (*w/v*), at 90 °C; then glycidyl methacrylate (GMA) was added to the mixture, with a final concentration of 7% (w/v), at 50 °C. The reaction was carried out for 48h at 50 °C while the pH of the solution was adjusted at 8.0 by adding 1 M NaOH solution. The resulting

solution was dialyzed in distilled water using dialysis tubes (12.000 × 14.000 Da cut off) at 4 °C for 5 days. Finally, the solution was freeze-dried to obtain pure GGMA. The derivatization degree (DD) of the obtained GGMA, determined by ^{1}H NMR analysis, previously defined in (Severini et al., 2023), is 0.014 ± 0.001.

2.3. Hydrogel preparation

GG and GGMA hydrogels were prepared following the same protocol as ref. (Iannuccelli & Sotgiu, 2010; Matricardi et al., 2009; Mazzuca et al., 2014; Mazzuca et al., 2016). Pure or methacrylate GG was dispersed in ultrapure water under stirring at room temperature. The amount of GG powder was weighed according to the final desired concentration. Since gelation mechanism is influenced both by temperature and by the presence of cations in water that makes the gel hard and brittle with a more ordered "crystalline-like" structure (Iannuccelli & Sotgiu, 2010), a proper amount of sodium chloride (NaCl) or calcium acetate ($Ca(CH_3COO)_2$, Ac_2Ca) solution (1 M) was added to the solution to obtain the established salt concentration, C_s. The resulting mixture was heated rapidly to the boiling point becoming transparent, then the homogeneous solution was poured into the Petri dishes and left to cool at room temperature for at least an hour. In this work pure GG hydrogels were prepared at different weight concentrations (C_w = 0.5%, 1.0%, 1.5%, 2.0%, 2.5%, 3.0%, 4.0%, 5.0%) while GG hydrogels with the addition of NaCl (C_{NaCl} = 0.5, 2.5, 5.0, 27.0 mM) or of Ac_2Ca (C_{Ac_2Ca} = 0.25, 1.25, 2.5, 5.0 mM) were also prepared at fixed GG concentration C_w = 2.0%. In addition, GGMA was also prepared at C_w = 2.5% with the addition of Ac_2Ca (C_{Ac_2Ca} = 5.0 mM). The reason for this choice was to obtain a GGMA sample with rheological characteristics similar to pure GG at C_w = 2.0%, chosen as a reference, as described in more detail by ref. (Severini et al., 2023). It should be pointed out that the concentrations of monovalent ion (NaCl) and divalent one (Ac_2Ca) have been chosen in order to be able to compare results obtained keeping constant the total charge concentration. In this way, it is possible to directly evaluate the effect of monovalent and divalent cations on gel formation.

2.4. Microgel preparation

The preparation protocol of gellan gum microgels described in ref. (Di Napoli et al., 2020) has been here improved thanks to the use of an Anton Paar MCR102 rheometer (Anton Paar Group AG, Graz, Austria). Unlike the previous method, where the GG solution was prepared in a beaker with the help of a magnetic stirrer and heated in a water bath using a manually controlled hot plate (aiming to maintain the raising temperature rate of 0.5 °C/min), the preparation process is now automated using a rotational rheometer. This ensures a more precise and consistent temperature and stirring control during the preparation, which is fundamental for the reproducibility of the sample preparation, ensuring that gelation occurs exactly in the same way. Pure GG and GGMA microgels were prepared dispersing a few milligrams of GG powder in ultrapure water in a glass beaker at room temperature under stirring (with a magnetic stirrer), covering the beaker with aluminium foil to prevent evaporation, as also described in ref. (Caggioni et al., 2007; Di Napoli et al., 2020; D'Oria et al., 2024).

The dispersion of GG in water was transferred into a custom-made 50 mm diameter bottomless silicone cylinder, enabling direct deposition of the sample onto the rheometer plate. A 50 mm diameter cone was used to shear the sample at a gap of about 3.5 cm. The solution was heated up to T = 80 °C, under the application of a constant shear rate of 500 s^{-1} and left for 10 min in this condition. An opportune aliquot of concentrated NaCl solution (1 M) was added, with a Gilson pipette, to obtain the chosen salt concentration C_s and promoting the gelation process before cooling. The viscosity trend was followed during both the heating and cooling stages. GG and GGMA microgels were prepared at C_w = 0.1%, C_w = 0.2%, 0.3%, 0.5% at fixed NaCl concentration C_{NaCl} = 100 mM.

2.5. Rheological measurements

Rheological measurements were carried out with a rotational rheometer Anton Paar MCR102 with a cone plate geometry (plate diameter = 49.97 mm, cone angle = 2.006°, truncation = 212 μm). Temperature was controlled using a Peltier system equipped with an evaporation blocker and an isolation hood to prevent evaporation. Rheological measurements on GG and GGMA hydrogels and microgels at different weight and salt concentrations were performed both in oscillatory and in steady shear regimes. Amplitude sweep measurements of $G'(\gamma)$ and $G''(\gamma)$ vs shear strain γ were used to determine the extent of the linear viscoelastic region (LVR) and the critical onset of non linearity. They were carried out in the strain range γ = (0.01–100)% at fixed frequency. Frequency sweep tests of $G'(\omega)$ and $G''(\omega)$ vs frequency $f = \omega/2\pi$ were performed in the frequency range f = (0.01–100) Hz at an applied strain γ small enough to ensure that it is in linear viscoelastic regime where most of viscoelastic materials behave linearly with direct proportionality between the stress σ and the deformation γ. These measurements were performed to assess the effects on the mechanical spectra. Temperature sweeps of $G'(T)$ and $G''(T)$ vs temperature were carried out to assess the sol-gel transition of both GG hydrogels and microgels in the temperature range (25–100) °C depending on the sample.

2.6. Dynamic light scattering (DLS) measurements

The particle hydrodynamic radius R_h has been measured through Dynamic Light Scattering (DLS) as a function of temperature. An optical setup based on a solid state laser (100 mW) with monochromatic wavelength λ = 642 nm and polarized beam has been used to probe samples in dilute regime. Measurements have been performed at a scattering angle θ = 90° that corresponds to a scattering vector Q = $(4\pi n/\lambda)\sin(\theta/2)$ = 0.018 nm^{-1} where n = 1.33 is the solvent (water) refractive index. The hydrodynamic radii have been obtained through the Stokes-Einstein relation:

$$R_h = k_B T / 6\pi\eta_s D_t \quad (1)$$

where k_B is the Boltzmann constant, η_s the viscosity of the solvent, namely water, at the measured temperature and D_t the translational diffusion coefficient related to the relaxation time τ through the relation:

$$\tau = 1/(Q^2 D_t). \quad (2)$$

The relaxation time was obtained by fitting the autocorrelation function of scattered intensity through the Kohlrausch-William-Watts expression (Kohlrausch, 1854; Williams, 1970):

$$g_2(Q,t) = 1 + b\left[exp\left(-(t/\tau)^{\beta}\right)\right]^2 \quad (3)$$

with the stretching exponent β providing the deviation from the single exponential. The decay of the autocorrelation function provides insights into the diffusion behaviour of microgels. A slower decay implies a longer relaxation time, showing slower dynamics due to increased interaction and frictional forces from larger hydrodynamic radii. Conversely, a faster decay indicates smaller size and quicker diffusion rates.

To ensure a constant temperature, the samples were kept at T = 25 °C for 5 min before measurements.

3. Results and discussion

3.1. Hydrogels rheological characterization

3.1.1. Pure GG hydrogels characterization

We start by reporting the rheological behaviour of pure GG hydrogels at different weight concentrations and salt content with the aim to understand the viscoelastic properties as the polysaccharide content increases. Although this problem has been investigated before, the weight concentration of GG has not reached large enough values as required by the use for paper cleaning in the cultural heritage field (Puoti et al., 2017). Amplitude sweep experiments were carried out to estimate the dynamic linear viscoelastic range in oscillatory shear strain. Fig. 1(a) illustrates the storage, GG$'(\gamma)$, and loss, G$''(\gamma)$, moduli of pure GG hydrogels at different concentrations, at f = 1 Hz and T = 25 °C, as a function of shear strain γ. At the lowest concentration, C_w = 0.5%, G$''(\gamma)$ is greater than G$'(\gamma)$ over the entire strain range, typical behaviour of a liquid-like system. With increasing concentration the trend is reversed and at approximately C_w = 1.0%, G$'(\gamma)$ becomes greater than G$''(\gamma)$, followed at larger concentrations by an increase of the moduli of several orders of magnitude, indicating the onset of solid-like behaviour. Interestingly, the onset of non-linear response is detected at the highest studied concentrations, i.e., C_w = 3.0% and 4.0%. In particular, G$''(\gamma)$ displays a peak whose maximum corresponds to the inversion point of the moduli and to a decrease of G$'(\gamma)$. This occurs at the so-called breaking point, characterized by the yield strain γ_c (arrows in Fig. 1 (a)), which is found to shift to smaller values as C_w increases, suggesting the presence of a more rigid and brittle structure. To define γ_c, we use the intersection between G$'(\gamma)$ and G$''(\gamma)$, following literature. Recently, the increase of the loss modulus at the onset of non-linear dynamic response has been related to energy dissipation associated to microstructure reorganization before collapsing under shear (García et al., 2011; García et al., 2016) and also qualitatively connected to the strength of the network in response to increasing deformation (Calero et al., 2010; García et al., 2011). Additional measurements are reported in Fig. S1 of the Supplementary Materials.

Plateau moduli $G_0'(\gamma)$ and $G_0''(\gamma)$, obtained at low strain γ = 0.1% in the linear viscoelastic region, are reported in Fig. 1(b) as a function of concentration, showing an increasing trend with C_w, in agreement with previous studies (Clark, 1992; Rodríguez-Hernández et al., 2003) performed in a concentration range from 0.005% to 0.05%, albeit significantly lower than the present one. The breaking point γ_c as a function of concentration, in Fig. 1(c), decreases with increasing concentration. The trend is well described by a decreasing exponential, reaching a plateau value γ_c =(1.8–1.9)% at high concentrations. This indicates that from a threshold concentration value of about 3.0% the microscopic polysaccharide structure has similar brittle properties. The figure showing the moduli as a function of frequency is provided in Fig. S2 of the SI and is consistent with the behaviour of the amplitude sweep, confirming our observations. At C_w = 1.0%, the system is in a fluid state as shown in Fig. 1(a); however G$'(\gamma)$ > G$''(\gamma)$ over the entire frequency range indicating a dominant elastic behaviour. At concentrations C_w = 2.0% and 3.0%, G$'(\gamma)$ and G$''(\gamma)$ are almost independent on frequency and G$'(\gamma)$ is higher than G$''(\gamma)$, typical hallmark of a solid like behaviour. The observed trend with concentration supports the increase of gel domains with increasing concentration, in agreement with what reported in ref.

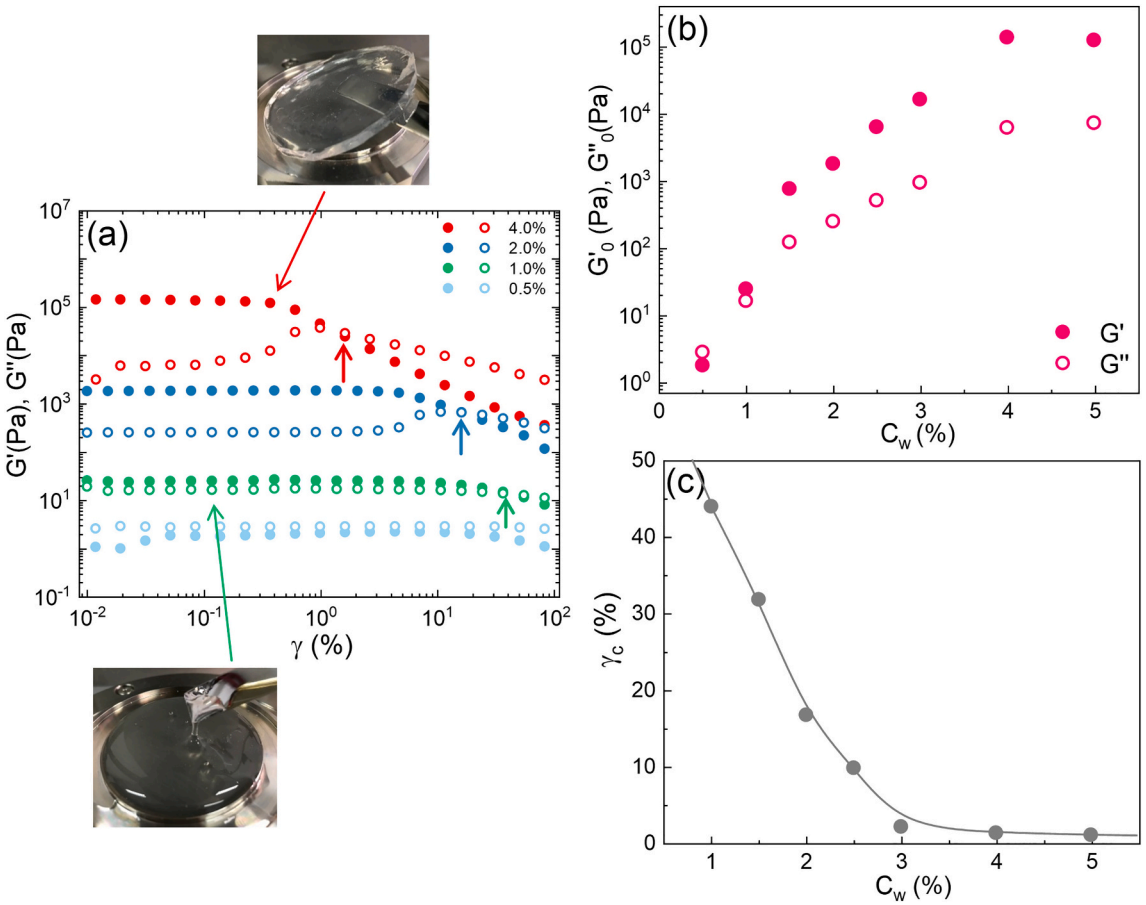

Fig. 1. (a) Storage G$'(\gamma)$ (closed circles) and loss G$''(\gamma)$ (open circles) moduli as a function of shear strain γ, at f = 1 Hz and T = 25 °C for pure GG hydrogels at four different concentrations (0.5% light blue, 1.0% green, 2.0% blue and 4.0% red), with related photographs of GG in the fluid and in the solid states. Short arrows indicate the breaking point γ_c. (b) Plateau moduli $G_0'(\gamma)$ and $G_0''(\gamma)$ and (c) breaking point γ_c as a function of GG concentration.

(García et al., 2011), in which, however, only very low concentrations from 0.025% to 0.25% were investigated.

3.1.2. Sol-gel transition of GG hydrogels

As mentioned above, the gelation process of GG is a complex phenomenon influenced by many factors, including the physicochemical properties of the solvent, temperature, and ionic concentration. In physical gels such as the present ones, an accurate detection of the sol-gel transition can be experimentally challenging. Gellan gum gelation is commonly described as a two-step thermoreversible process with an initial helix ordering, followed by the association between stiff double helices through intermolecular interactions (Grasdalen & Smidsrød, 1987; Safronov et al., 2018), recently confirmed by molecular dynamics simulations (Tavagnacco et al., 2023). Typically, gelation in GG systems occurs by decreasing temperature and/or by increasing ionic concentration (Pérez-Campos et al., 2012). Here, we first focus on the temperature behaviour by performing dynamic moduli measurements versus temperature during gelation, as reported in refs. (Dai et al., 2008; Dai et al., 2010; Pérez-Campos et al., 2012; Tako et al., 2009). The gel point temperature, T_c, is defined as the temperature where the moduli cross over. According to it, by monitoring the temperature evolution of the moduli during cooling at fixed frequency (f = 1 Hz, ω = 6.28 rad/s), we can obtain an estimate of the gel point as the crossover point of $G'(T)$ and $G''(T)$, corresponding to $\tan\delta = 1$, later followed by a trend inversion whereby $G''(T) < G'(T)$. In Fig. 2(a) the temperature dependence of dynamic moduli and $\tan\delta$ during the cooling process (2.0 °C/min) is reported for GG samples at concentrations: C_w = 1.0%, 2.0% and 4.0% highlighting the onset of gelation. At the lowest concentration, 1.0%, gelation occurs for $T_c \sim 80$ °C while at 2.0% this occurs upon cooling already approximately ~ 93 °C. Further increasing GG concentration to 4.0%, no intersection between dynamic moduli is detected, with $G'(T)$ always being larger than $G''(T)$ throughout all the cooling range. This indicates that gelation in this case is instantaneous as soon as the heating process is stopped and the sample start to cool. An increase of the plateau of the moduli can be observed when temperature further decreases below the gel point ($T < T_c$). This trend may be due to the fact that the aggregation of double helices into the ordered conformation of GG is not energetically preferred at temperatures just below T_c, while lower temperatures enhance their formation. Fig. 2(b) reports the moduli, together with their respective $\tan\delta$ for the sample at C_w = 2.0% to highlight that they overlap in correspondence of the gel point where $\tan\delta = 1$.

Nonetheless, it has been argued that the temperature corresponding to the crossover, T_c, may vary depending on the frequency (Pérez-Campos et al., 2012) at which moduli are measured and therefore it cannot be really considered an effective sol-gel transition temperature, T_{gel}, although very close to T_{gel}. Following the work by Winter and Chambon (Winter & Chambon, 1986), an interpolation method can be implemented, known as the critical phase angle procedure where $\tan\delta$ is frequency independent. The convergence point of the tangent at various angular frequencies determines the gelling temperature, T_{gel}. In Fig. 2(c) the temperature dependence of $\tan\delta$ of pure GG is shown for different angular frequencies at C_w = 2.0%. The convergence point of all frequencies is found to be at T_{gel} = 97.4 °C, corresponding to the point where the critical phase angle δ becomes frequency independent. This value is slightly greater, but quite close to T_c = 93.6 °C, so that the latter can be considered as a good approximation to the gel point. Overall, these measurements indicate that the best suitable GG hydrogel without salts for cultural heritage purpose is that with C_w = 2.0%: it could indeed withstand a pressure up to 1000 Pa without breaking (see Fig. 6).

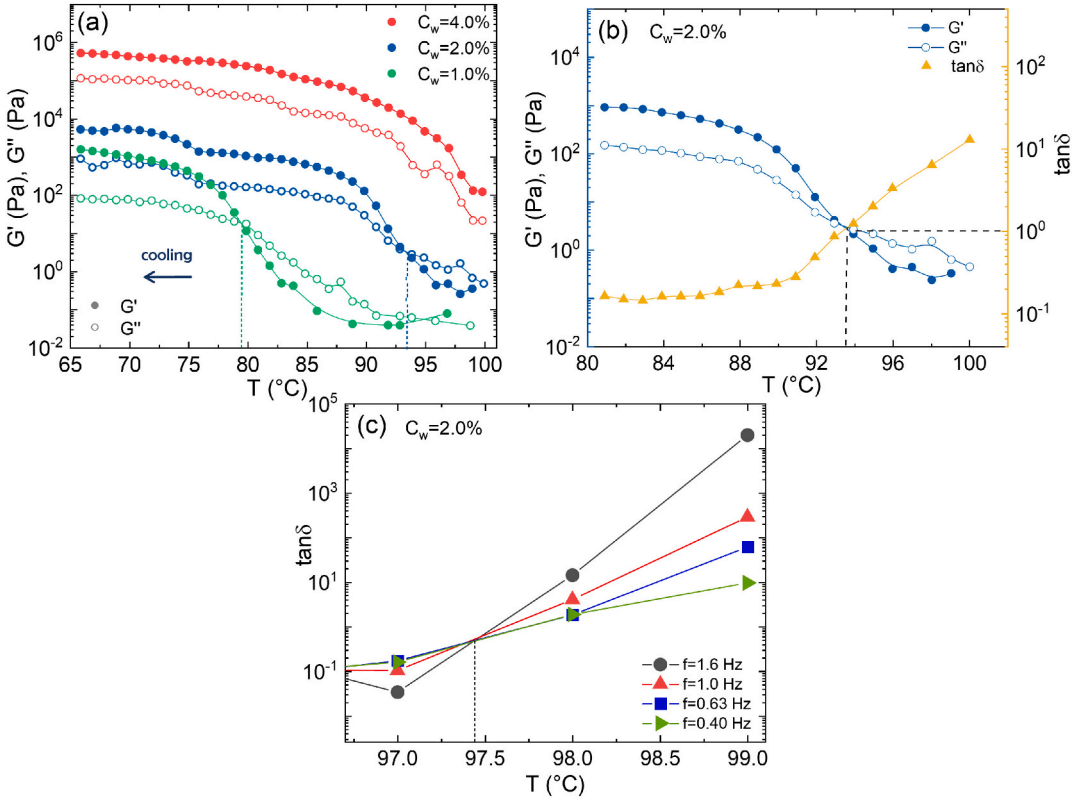

Fig. 2. (a) Temperature evolution of $G'(T)$ (closed circles) and $G''(T)$ (open circles) during cooling for pure GG at a rate of 2.0 °C/min, at f = 1 Hz and at C_w = 1.0% (green), 2.0% (blue) and 4.0% (red). (b) Temperature dependence of the moduli and $\tan\delta$ (orange triangles) for pure GG at C_w = 2.0 %. The crossover point defines T_c = 93.6 °C. (c) Temperature dependence of $\tan\delta$ for pure GG at different angular frequencies: f = 1.6 Hz (grey circles), f = 1.0 Hz (red triangles), f = 0.63 Hz (blue squares) and f = 0.40 Hz (green triangles). The crossover point defines T_{gel} = 97.4 °C according to the critical phase angle procedure (Winter & Chambon, 1986).

3.1.3. Characterization of GG hydrogels in presence of salts

The gelation mechanism of GG has been widely discussed in literature (Diener et al., 2019; Diener et al., 2020; Grinberg et al., 2003; Tavagnacco et al., 2023). It is assumed that in the second step of gelation, the presence of salts promotes the formation of a gel, affecting the double-helix structure because of electrostatic interactions with cations. In particular, the mechanical properties of GG in the presence of different salts have suggested that double helices aggregation follows distinct mechanisms in the presence of monovalent or divalent cations (Tavagnacco et al., 2023). For divalent ions at a given ionic concentration, GG hydrogels are firmer and harder than those prepared with monovalent ions (Miyoshi et al., 1996; Rodríguez-Hernández et al., 2003) doubling ionic concentration so as to maintain constant the total charge concentration. Here, we complement this evidence for the gels used for paper cleaning applications. In particular, we perform rheological measurements by adding different amounts of NaCl and Ac_2 Ca salts to GG to form hydrogels. These are compared with the corresponding results for pure GG, keeping its concentration constant at $C_w =$ 2.0%, which is the one that was found to perform the best in the paper cleaning tests (Mazzuca et al., 2014).

In Fig. 3, we report $G'(\gamma)$ and $G''(\gamma)$ vs γ for different GG hydrogels prepared in the presence of varying divalent, salt Ac_2Ca (Fig. 3(a)(c)), and monovalent one, NaCl, amount (Fig. 3(b)(d)). The addition of salts leads, in both cases, to an increase of $G'(\gamma)$ of one order of magnitude with respect to pure GG hydrogel as shown in Fig. 3 (a) (b); however the behaviour of hydrogels are quite different for the two cases. Indeed, in the presence of divalent cations, with increasing Ac_2Ca concentration, a continuous increase of $G'(\gamma)$ is observed, while for NaCl a sudden change with respect to pure GG is obtained at the lowest investigated salt concentration, without further increase even at the highest NaCl investigated concentration. This is in qualitative agreement with molecular dynamics simulations, which pointed out that divalent salt is able to efficiently bridge GG chains into aggregated double helices, while monovalent ions cannot act as effective linking agents, but can only increase the screening between the GG chains. Therefore, their role is not prominent and cannot be used as a control way to obtain hydrogels of the desired stiffness. Similar results are observed for the loss moduli $G''(\gamma)$ in Fig. 3 (c) (d), where a peak that is larger and shifted to lower strain, is found with increasing Ac_2Ca content, while the corresponding behaviour for NaCl is independent of the actual salt concentration. An additional comparison is reported in Fig. S3 of the Supplementary Materials, where $G'(\gamma)$ and $G''(\gamma)$ vs strain and frequency, of GG hydrogels at fixed concentration $C_w = 2.0\%$, without and with NaCl (5 mM) and Ac_2Ca (2.5 mM) are compared with those of pure GG hydrogel. Altogether, these results confirm that the viscoelastic behaviour of GG hydrogels is influenced much more strongly by divalent cations than by monovalent cations, as reported in ref. (Miyoshi et al., 1996), where the authors compared the effect of KCl, NaCl, $CaCl_2$ and $MgCl_2$ concluding that divalent cations promote the formation of thermally stable junction zones. To better visualize this effect, the plateau moduli at low strain values are shown as a function of salt concentration C_{salt} for GG with Ac_2Ca (red circles) and NaCl (orange squares) in Fig. 4(a). Furthermore, in Fig. 4(b) the critical strain γ_c is reported, showing a smooth decrease with increasing C_{salt} for GG in the presence of Ac_2Ca, which favors closer

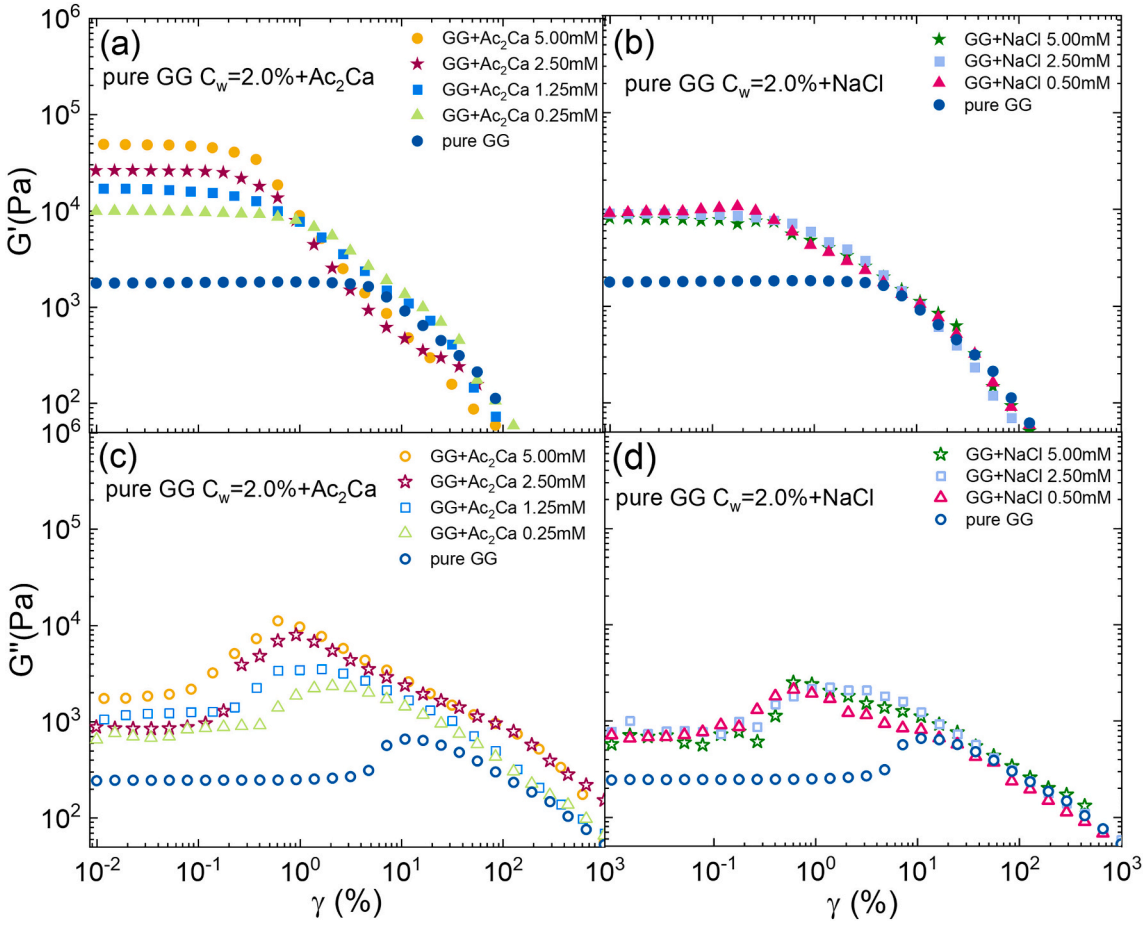

Fig. 3. (a) (b) Storage $G'(\gamma)$ (closed circles) and (c) (d) loss $G''(\gamma)$ (open circles) moduli as a function of shear strain γ at $T = 25$ °C at $C_w = 2.0\%$ with different Ac_2Ca contents (0.25 mM (light green triangles), 1.25 mM (light blue squares), 2.50 mM (purple stars) and 5.00 mM (orange circles)) or NaCl contents (0.500 mM (pink triangles), 2.50 mM (light violet squares), and 5.00 mM (green stars)), compared with pure GG (blue circles).

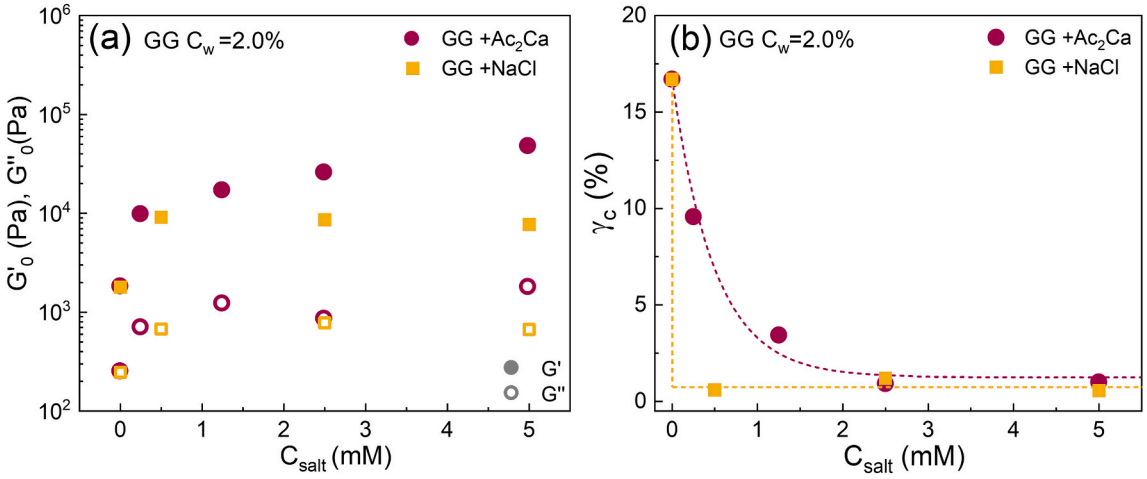

Fig. 4. (a) Plateau moduli $G'_0(\gamma)$ and $G''_0(\gamma)$ at $\gamma = 0.1\%$ and (b) breaking point γ_c as a function of C_{salt} for GG hydrogels at $C_w = 2.0\%$ with Ac_2Ca salt (red circles) and NaCl (orange squares). Lines are guides to the eye.

and tighter bindings between the chains at variance with NaCl. Finally for this section, we report in Fig. 5 the comparison of $G'(\gamma)$ and $G''(\gamma)$ at $C_w = 2.0\%$ for pure GG hydrogel and for GG hydrogels with different concentrations of Ac_2Ca and NaCl, but in such a way to keep constant the ionic strength (normality) in the different samples. Fig. 5(a) and (d) show that a very similar sample response is obtained at low salt content, despite using different monovalent or divalent salts. Interestingly, in the presence of a relatively high salt content, we find a quite pronounced variation of the moduli, as shown in Fig. 5(c) and (f). It should be noted that in literature the GG hydrogels with salts used for cultural heritage purpose contain Ac_2Ca = 2.50 mM, and therefore fall in this last category.

The effect of divalent cations is further revealed by looking at the stress reported in Fig. 6, where we compare shear stress value σ as a function of shear strain γ of the hydrogels without added salt (a), with calcium ions (b) and with sodium ions (c), separately. Strikingly, we find that in the presence of divalent ions, evidence of two-step yielding behaviour is observed, right at the conditions where we use these GG hydrogels for paper cleaning. Two-step yielding is associated with the occurrence of the breaking of the gel in two distinct processes (Ahuja et al., 2020). Here, we can hypothesize that at first the breaking of the cation-mediated aggregation of double helices occurs, followed by the breaking of the double helixes themselves. The two steps are separated by a difference in stress of roughly one order of magnitude (from about σ=110 Pa in the first step to σ=1100 Pa in the second step). Our cleaning tests, reported in literature (Mazzuca et al., 2014; Micheli et al., 2016),

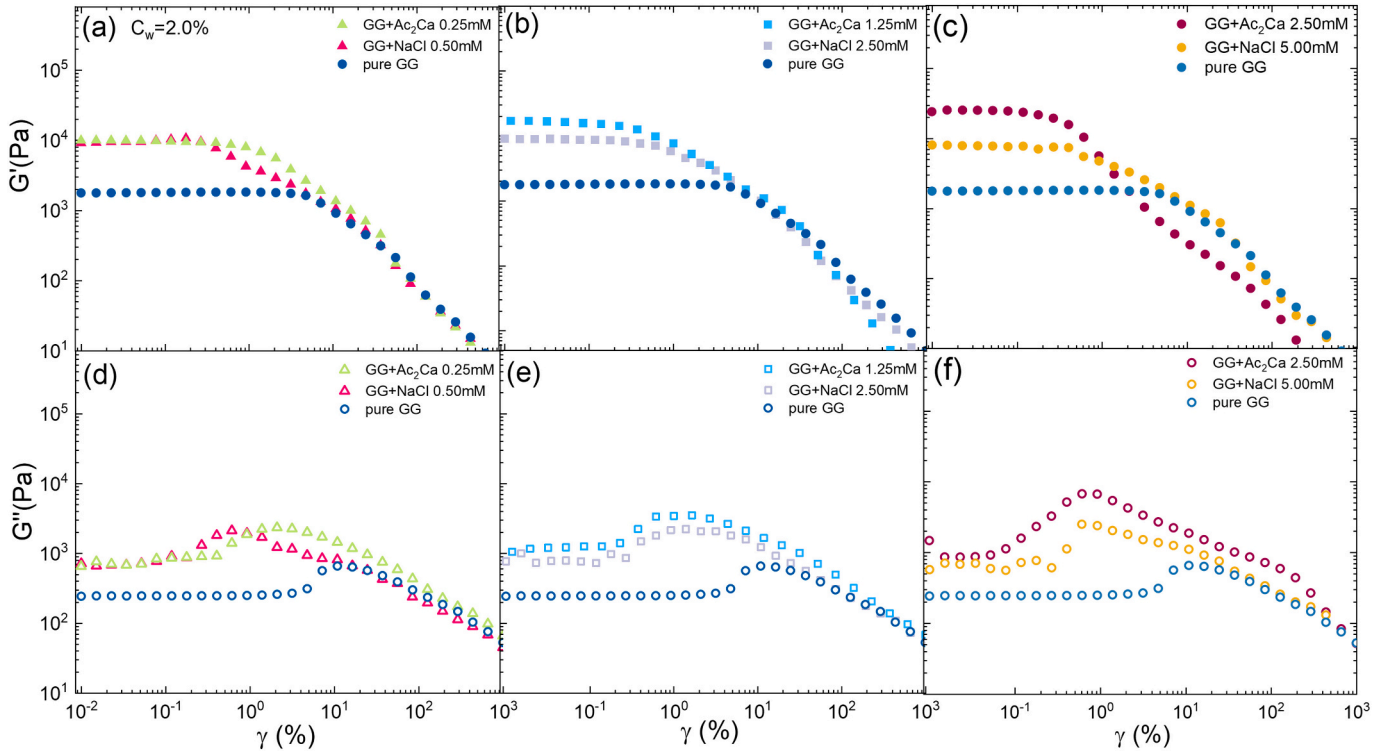

Fig. 5. (a) (b) (c) Storage $G'(\gamma)$ and (d) (e) (f) loss $G''(\gamma)$ moduli vs shear strain γ at $T = 25$ °C and $C_w = 2.0\%$ for pure GG hydrogel and for GG hydrogel with Ac_2Ca and NaCl at salt concentrations such as to keep constant the total charge concentration in the sample. (a; d): [Ac_2Ca] = 0.25 mM or [NaCl] =0.50 mM; (b,e): Ac_2Ca] = 1.25 mM or [NaCl] =2.5 mM; (c,f): Ac_2Ca] = 2.50 mM mM or [NaCl] 5.0 mM.

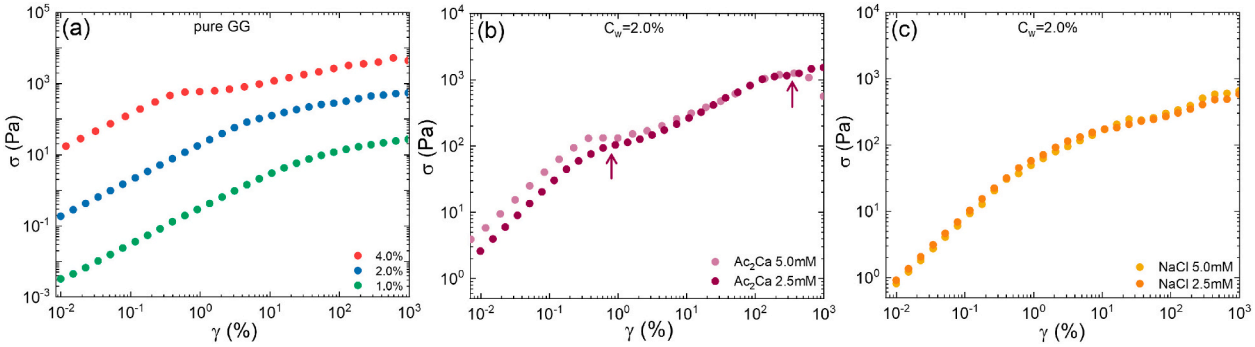

Fig. 6. Shear stress σ as a function of shear strain γ, at f = 1 Hz, T = 25 °C for (a) pure GG hydrogel at different concentrations and for GG hydrogels at C_w = 2.0% (b) with Ac_2Ca and (c) NaCl added salts. The arrows in (b) indicate the double yielding for the sample which best performs in paper cleaning.

definitely exclude that the gel leaves residues on paper, when pressures of the order a few hundreds Pa are exerted, while residues can remain on paper if pressure of thousands of Pa are put on the gel. Therefore, we deduce that gel is able to perform its cleaning function up to the second yielding point, with the presence of divalent cations giving it the necessary rigidity to be removed afterwards without any leaving residues. Instead, we do not observe double yielding in the presence of monovalent salt at the same normality, which confirms the fact that these cannot be used for cultural heritage purposes, since they are too soft and they can break after the weight is applied to it, leaving residues on paper sheets after process. Interestingly, double yielding also occurs for pure GG hydrogel at higher C_w, about 4.0% signaling that the presence of two-step yielding is intrinsic in the complex gelation process of GG, again depending on the particular conditions employed.

3.1.4. Sol-gel transition of GG hydrogels with cations

It is interesting to analyze the sol-gel transition of GG in the presence of salts. As discussed above, the addition of cations (monovalent or divalent ones) largely affects the viscoelastic behaviour of GG, as evident from the increase of the moduli by some orders of magnitude. This suggests that, in this condition, gelation should occur at lower GG concentrations in the presence of cations. Based on these premises, we investigate the gelation process of 0.5% GG samples with the addition of Ac_2Ca and NaCl salts at the same ions number cases. In Fig. 7, $G'(T)$ and $G''(T)$ versus temperature during the gelation process at cooling rate

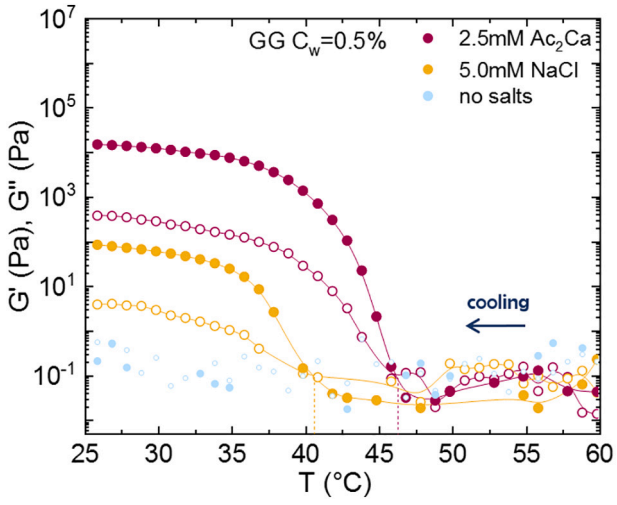

Fig. 7. Temperature evolution of $G'(T)$ (closed symbols) and $G''(T)$ (open symbols) during cooling at rate 2.0 °C/min at frequency 1 Hz of GG at C_w = 0.5% without salts compared with GG with 2.5 mM of Ac_2Ca and 5.0 mM of NaCl. The crossover point defines T(GG with NaCl) = 40.5 °C and T(GG with Ac_2Ca = 46.2 °C.

2.0 °C/min and frequency f = 1 Hz are reported at C_w = 0.5% for pure GG, GG with Ac_2Ca 2.5 mM and GG with NaCl 5.0 mM. First, we observe that at this low concentration, as discussed in the related section, pure GG remains liquid in the whole investigated temperature range, as evident from the low values of the moduli, whereas the addition of salts promotes gelation already at this low C_w. Interestingly, we observe that in the case of added Ac_2Ca, the inversion of the moduli occurs at slightly higher temperature, T = 46.2 °C, as compared to GG with NaCl, T = 40.5 °C, signaling that upon cooling the divalent ions are more effective in inducing gelation.

Importantly, low temperature plateaus of $G'(\gamma)$ and $G''(\gamma)$ increase by one and two orders of magnitude with respect to pure GG in the case of NaCl and Ac_2Ca, respectively. These findings further confirm the prominent role of cations in general and of divalent ones in the viscoelastic behaviour of GG hydrogels (Miyoshi et al., 1996; Tavagnacco et al., 2023).

3.1.5. Chatacterization of methacrylated gellan gum (GGMA) hydrogels

Finally, we focus on the chemical modification to gellan gum by methacrylation. This is because, the introduction of methacrylic groups allows to obtain hydrophobic gel, yielding a gel that is capable of removing both hydrophilic (i.e. cellulose degradation products) and hydrophobic substances with a single water-based treatment (Severini et al., 2023), a novel feature in paper cleaning procedures. In this case, based on results previously reported concerning the best hydrogels for paper cleaning, we focus here on methacrylated GG with the addition of Ac_2Ca only, having established in the previous section that this salts yields superior gels with respect to NaCl.

To characterize the rheological properties of these chemically-modified hydrogels, we report in Fig. 8 a comparison among pure GG, GG with 5.0 mM of Ac_2Ca and methacrylated gellan gum (GGMA) with the same content of salt and polymer concentration of C_w = 2.5%. Also in the case of GGMA, the addition of Ac_2Ca causes an increase of $G'(\gamma)$, suggesting a more tight structure between the chains and a more rigid gel. The slight difference in used C_w is due to the fact that after various attempts described in ref. (Severini et al., 2025), we found that a slightly larger amount of polymer is needed in the case of GGMA, i.e., C_w = 2.5% (versus C_w = 2.0% for pure GG) to obtain the same optimal hydrogel performance for paper cleaning. This is confirmed by the lower elastic moduli observed for GGMA with respect to the corresponding pure GG in Fig. 8. The trend of the plateau moduli $G'_0(\gamma)$ and $G''_0(\gamma)$ and of the critical strain γ_c with increasing GG concentration, with and without Ac_2Ca and GGMA with the same salt is shown in Fig. 9. Notably, we find that the two hydrogel formulations which are found to best perform in paper cleaning, namely GG at C_w = 2.0% with Ac_2Ca 5 mM and GGMA at C_w = 2.5% with Ac_2Ca 5 mM, have comparable elastic properties, as highlighted by the horizontal line in Fig. 9(a).

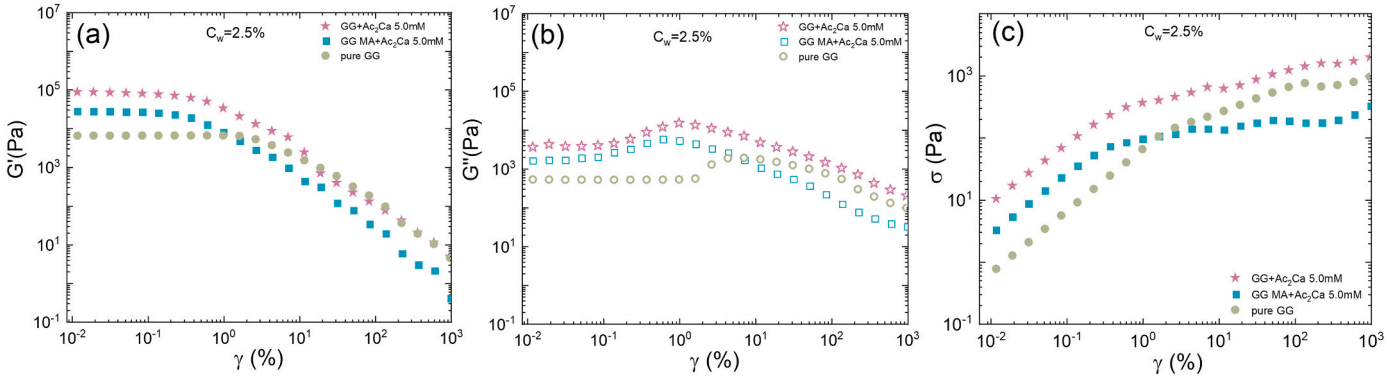

Fig. 8. (a) $G'(\gamma)$, (b) $G''(\gamma)$ and (c) σ vs shear strain γ at $T = 25$ °C and $C_w = 2.5\%$ for pure GG hydrogel, GG hydrogel with 5.0 mM of Ac_2Ca and methacrylate GG hydrogel with the same content of salt.

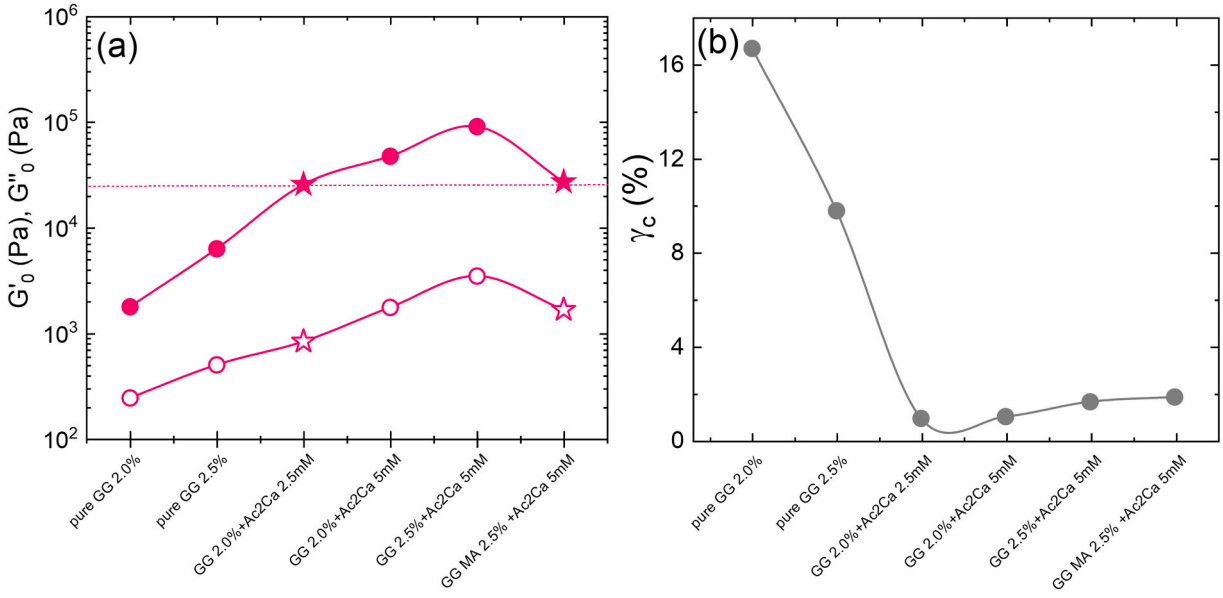

Fig. 9. Comparison of (a) the plateau moduli $G_0'(\gamma)$ (closed circles) and $G_0''(\gamma)$ (open circles) and (b) γ_c for the different GG and GGMA hydrogels tested, varying polymer and salt concentrations, at $T = 25$ °C. The horizontal line highlights the comparable value of G_0' obtained for the two hydrogels which best perform in paper cleaning.

3.2. Microgels characterization

3.2.1. GG microgels

Combining the promising features of microgels and the proven efficiency of GG hydrogels in removing impurities and degradation products from paper, GG microgels were developed with the aim of obtaining an innovative tool capable of improving the efficiency of currently available cleaning techniques for paper artworks (Di Napoli et al., 2020).

As reported in ref. (Di Napoli et al., 2020), GG microgels have been prepared and successfully employed, for the first time, in paper cleaning. Thanks to their reduced size, microgels have proven to be effective, providing a greater penetration into the porous structure of the paper adapting to the irregular surface of artefacts, with respect to hydrogels. Atomic Force Microscopy (AFM) images, reported in Fig. S1 of the Supplementary Materials, highlight the different structure of microgels and hydrogels. Thanks to their properties, microgels can clean very quickly, in the order of a few minutes, thus strongly minimizing time costs with respect to hydrogels (whose application can be up to two hours long).

We start this characterization by comparing the properties of GG microgels obtained with our initial preparation method, put forward in ref. (Di Napoli et al., 2020) and detailed in the Materials and Methods section, with those prepared in this work, thanks to the use of a rheometer, which allows for greater control over the produced samples. Fig. 10 shows the comparison of rheological measurements on the microgels obtained using the two methods. In Fig. 10(a) amplitude sweep results are conducted on two different sample preparations, both obtained with the initial preparation method. It is evident that, while the behaviour of the two samples is qualitatively similar, there is some differences in the measured values of the moduli. Conversely, the measurements carried out on two different samples prepared using the new rheometer-based method, in Fig. 10(b), are completely overlapped, indicating a significant improvement in consistency and reproducibility of the samples. We have verified that, in both cases, samples have the same cleaning efficacy, because despite small differences, microgels are able to efficiently and rapidly penetrate into the pores of the fibrous network of paper sheets, due to their small size, as will be discussed better below. In the following, all microgel results refer to samples prepared with the new method, as described in the Materials and Methods section, at the following GG concentrations: $C_w = 0.1\%$ (sample GG1), 0.2% (sample GG2), 0.3% (sample GG3), 0.5% (sample GG5). We

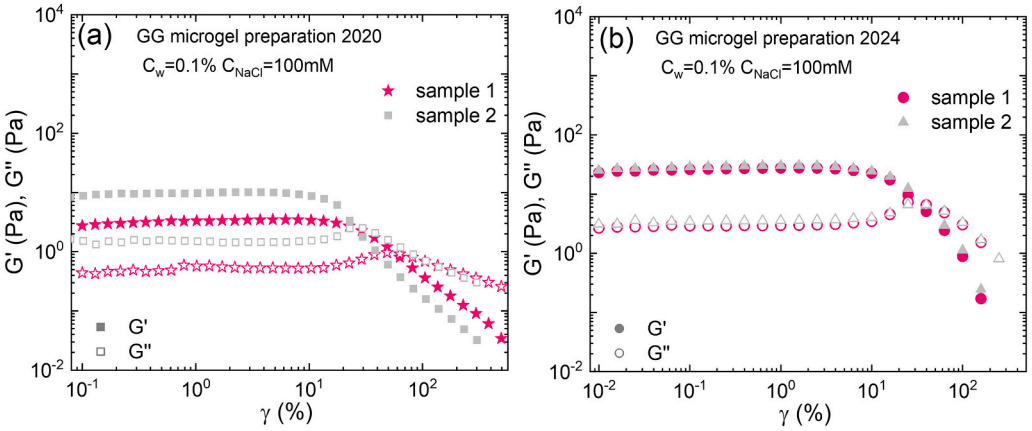

Fig. 10. Comparison between amplitude sweep measurements (storage modulus G′, closed symbols, and loss G″, open symbols vs shear strain γ), at f = 1 Hz, T = 25 °C in the case of microgels at C_w = 0.1% and C_{NaCl} = 100 mM prepared by (a) the old method published in 2020 (Di Napoli et al., 2020) and (b) the new rheometer-based method proposed in this work. In both panels two different samples (sample 1, pink colored and 2, grey colored) are compared for each method.

have analyzed that in detail the gelation process during microgel formation. In Fig. 11(a) the normalized viscosity of GG1 is reported as a function of temperature during the heating and cooling process under shear. During the initial heating, a quite linear decrease, most likely due to the chains forming double helix structures (Grinberg et al., 2003; Tavagnacco et al., 2023), is found. However, when cooling starts, a sudden increase of viscosity is observed at a temperature close to 40°, indicating the start of gelation where the double-helixes form networked structures (Diener et al., 2019; Grinberg et al., 2003).

In Fig. 11(a) the normalized viscosities vs temperature of the different GG microgels samples during the cooling process are also shown. The viscosity plateau value at low temperature increases with increasing concentration and a shift of the gelling temperature to higher values is observed, suggesting the development of more rigid gel structures. Gelling temperatures as a function of GG concentration, reported in Fig. 11(b), show that, at fixed salt content, samples with higher polysaccharide content, reach the gel state earlier during the cooling process. The normalized DLS autocorrelation functions measured in dilute condition (C_w = 0.01%) are reported in Fig. 11(c). They are directly correlated with the size of the particles through the Stokes-Einstein relation eq.1. In particular, the particle radii are shown in Fig. 11(d), together with the stretching parameter β. We find that the radii are always in the order of a few hundreds nanometers, with a slight decrease in size as GG concentration increases. In concurrence, there is a slight decrease of β, that is related to the polydispersity of the samples, that appear to be quite pronounced in comparison to standard microgel synthesized by precipitation polymerization or other techniques (Fernandez-Nieves et al., 2011). It is important to compare these results with those obtained with the old preparation method in ref. (Di Napoli et al., 2020), where the microgels were found to have a larger size (close to 1 μm radius) and a lower stretching index, close to 0.4. Hence, both methods yield microgels capable to clean well the paper artefacts. This is because, as explained earlier, the pores of paper are also quite polydisperse and hence, the fine details are not crucial for their efficacy (Corsaro et al., 2016): the key feature is truly the presence of a moderate polydispersity of the samples which allows them to better adapt to the rough paper surface.

To probe the viscoelastic properties of GGx microgels (where x is 1, 2, 3, or 5), storage and loss moduli were measured at 25 °C) as a function of shear strain and fixed frequency 1 Hz and ii) as a function of frequency

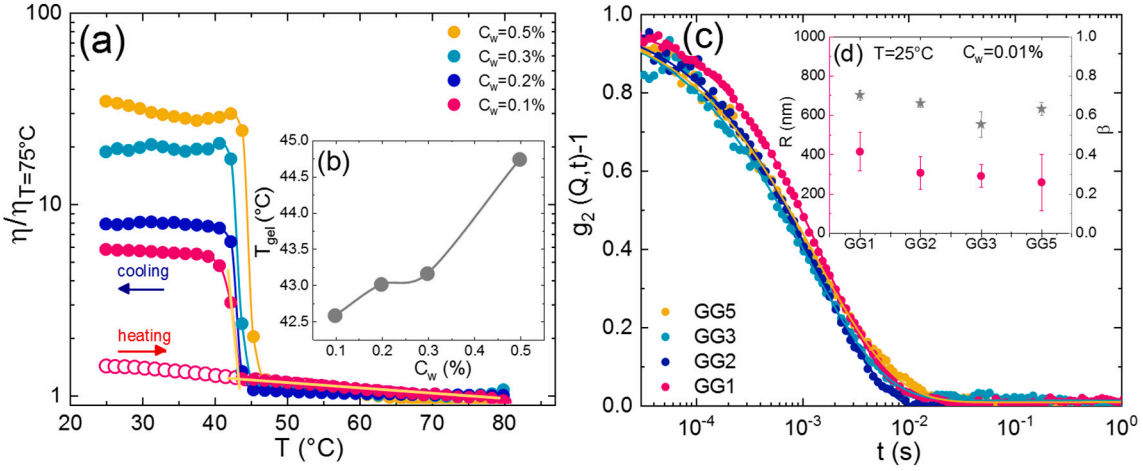

Fig. 11. (a) Normalized viscosity vs temperature during the two steps of microgel preparation: during cooling (indicated by the blue arrow) for GG microgel at C_w = 0.1%,0.2%,0.3% and 0.5% and during heating (indicated by the red arrow) for GG at C_w = 0.1%, under a constant shear rate of 500 s^{-1}. (b) Gelling temperature as a function of concentration, determined from the intersection point between the tangent at the base and at the midpoint height of the inflection of the curve (see orange curves drawn as an example for the C_w = 0.1% sample). (c) Normalized intensity autocorrelation function g_2(Q,t)-1 of GG1, GG2, GG3 and GG5 samples (corresponding to microgels prepared by the new method at GG at C_w = 0.1%,0.2%,0.3% and 0.5%) measured in dilute condition, at C_w = 0.01%, and θ = 90°, corresponding to Q = 0.018 nm^{-1}. (d) Hydrodynamic radius R (red circles) and stretching parameter β (grey stars) obtained from fits of g_2(Q,t) through the eq. 3, (see Materials and Methods section).

at fixed shear strain γ=0.1% in the linear viscoelastic region for all samples, as reported in Fig. 12(a) and (b), respectively. In Fig. 12(a), $G'(\gamma)$ is higher than $G''(\gamma)$ in the linear viscoelastic range, for all the samples, indicating that the elastic behaviour prevails over the viscous one. As the concentration increases, from GG1 to GG5, both $G'(\gamma)$ and $G''(\gamma)$ increase, suggesting a denser and more interconnected microgel structure. The breaking point, which marks the beginning of the non-linear response, shifts from y=30%, for the sample with low concentration (GG1) to y=3.0% for the more concentrated GG microgel (GG5) indicating that the microgel structure becomes more fragile as the concentration increases. In Fig. 12(b), $G'(f)$ remains higher than $G''(f)$ across the entire frequency spectrum, confirming the predominantly elastic nature of the microgel network which exhibits weak frequency dependence over the tested range, a typical behaviour for gel-like materials. The relative stability of the moduli across frequencies further indicates that the microgels maintain their structural integrity and viscoelastic properties, reinforcing their potential for applications requiring a consistent mechanical performance.

3.2.2. GGMA microgels

The last preparation protocol was adopted for preparing GGMA microgels at different polymer concentrations, keeping fixed the NaCl content at 100 mM, in order to find the GGMA concentration for obtaining microgels with rheological properties similar to the successfully tested GG one (C_w = 0.1%, C_{NaCl} = 100 mM) (Di Napoli et al., 2020). This strategy ensures similar gel properties and interactions with paper surface. We thus tested the following GGMA concentrations: C_w = 0.1% (sample GGMA1), 0.2 % (sample GGMA2), 0.3 % (sample GGMA3), 0.5 % (sample GGMA5).

In Fig. 13(a) we report the normalized viscosity vs temperature of the different samples during the cooling process. We observe a pronounced increase of viscosity with increasing GGMA concentration and a shift of the gelation to higher temperature, suggesting again the development of more rigid gel structures at higher polymer concentrations. Gelling temperatures as a function of GGMA concentration are reported in Fig. 13(b), showing that, similarly to pure GG microgels, samples with larger polysaccharide concentration and the same salt content reach, on cooling, the gel state first. The particle radii of the various GGMA samples, obtained by the DLS normalized autocorrelation functions, reported in Fig. 13(c) and in Fig. 14(d), are comparable to those observed for GG samples, also showing similar stretching index. Overall, these findings strongly support the idea that the adopted methacrylation procedure does not fundamentally alter the microgel structure, just providing an additional functionality which makes them suitable to interact more efficiently with hydrophobic compounds.

Next, we turn to discuss the storage and loss moduli vs shear strain, that are reported in Fig. 14 at f = 1 Hz and T = 25 °C for GGMA at different concentrations. Again, we find that $G'(\gamma)$ is greater than $G''(\gamma)$ for all samples and the plateau values increase with concentration, as in the case of pure GG microgels. There is a shift of the breaking point γ_c from about 40%, for the less concentrated sample (GGMA1), to 30 %, for the most concentrated sample (GGMA5). The displacement to lower γ of the beginning of the non-linear viscoelasticity zone with increasing polysaccharide concentration happens within a smaller range than for pure GG, suggesting that methacrylation makes it less susceptible to concentration changes. The stability of the sample over time was tested by comparing the amplitude sweep measurements of freshly prepared samples with those several hours after the preparation, as reported in Fig. S4(a) of the SI and (b) for two different concentrations. Comparing the values of the moduli with pure GG, we find that the sample with C_w = 0.2% GGMA is the most similar to C_w = 0.1% GG. Indeed, this sample was tested for paper cleaning in ref. (Severini et al., 2025) and its efficacy was found to be the same as that for pure GG microgels, but with the additional ability to remove hydrophobic residues. Finally, we compare the flow curves of the microgels in Fig. 15, for microgels (a) and for GGMA microgels (b), both as a function of polysaccharide concentration. Interestingly, despite the lower overall moduli with respect to the hydrogels, we also observe for microgels the emergence of double yielding, signaling that, independently of the internal arrangement in a macroscale network or in microspheres, the gelation mechanism is the same. Here, it is peculiar that the microgels are obtained in the presence of monovalent ions, for which hydrogels did not show the two-step yielding, pointing to a difference due to the shear-induced aggregation which seems to stabilize the micro-aggregates to a greater extent, making them more resistant to fracture. It is important to note that despite the low values of the stress observed here, the microgel-based cleaning protocol does not need the application of a weight and involves a removal step using water. This effectively limits the production of residues and makes them suitable for the desired purposes.

4. Conclusions

In this work, we comprehensively investigated the rheological properties of GG hydrogels and microgels, examining the effects of temperature, gellan concentration, methacrylation, the presence of different cations (Na^+, Ca^{2+}), and salt concentration on viscosity and viscoelastic moduli. The main results of our work can be summarized as follows.

We developed a reliable, shear-driven preparation protocol for producing GG microgels also in presence of methacrylation. This protocol,

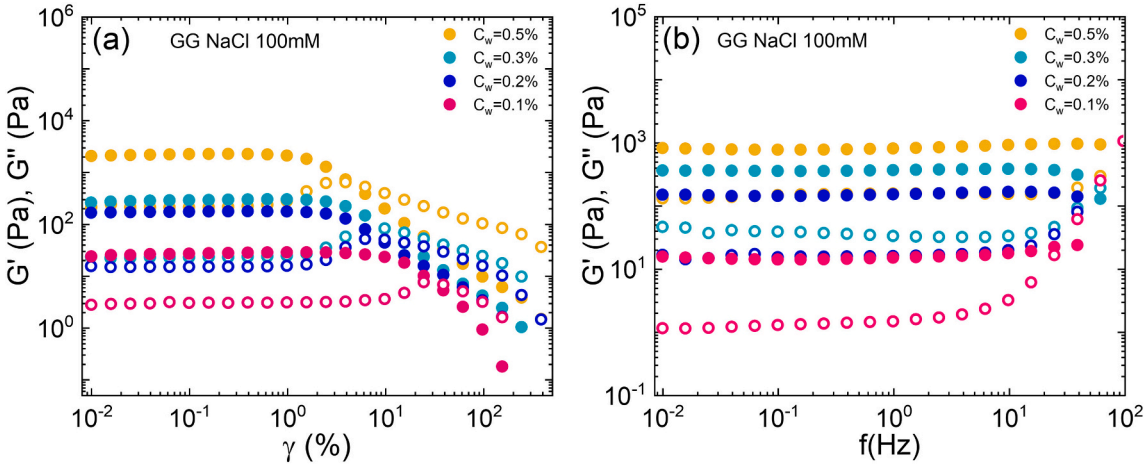

Fig. 12. (a) Storage G′ (closed circles) and loss G″ (open circles)moduli as a function of γ at f = 1 Hz and (b) as a function of frequency f at γ = 0.1% for GG microgels at different concentrations, T = 25 °C and C_{NaCl} = 100 mM.

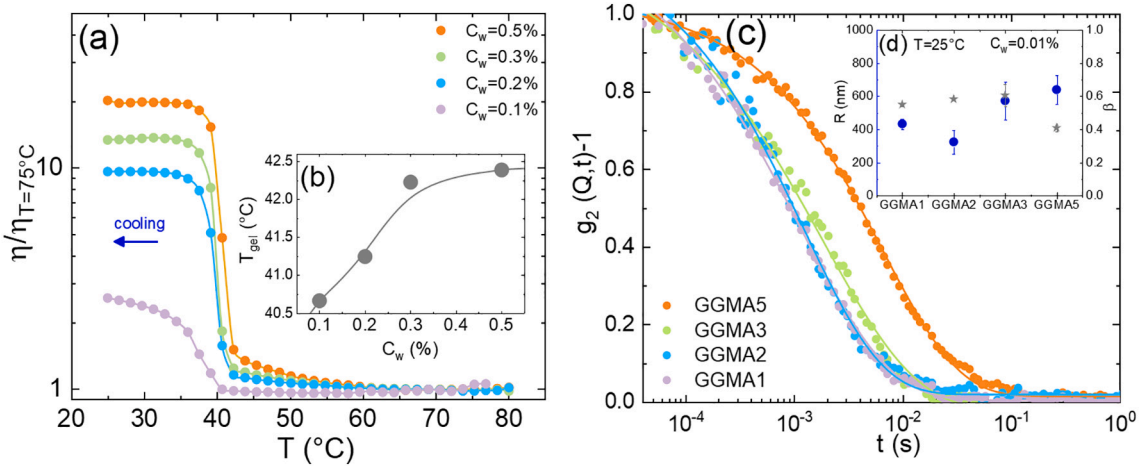

Fig. 13. (a) Normalized viscosity vs temperature during cooling (blue arrow) for GGMA microgels at C_w = 0.1%,0.2%,0.3% and 0.5% (called GGMA1, GGMA2, GGMA3 and GGMA5 respectively), under a constant shear rate of 500 s^{-1}. (b) Gelling temperature as a function of concentration. (c) Normalized intensity autocorrelation functions of GGMA1, GGMA2, GGMA3 and GGMA5 samples measured in dilute condition, at C_w = 0.01%, and $\theta = 90°$, corresponding to Q = 0.018 nm^{-1}. (d) Hydrodynamic radius and β obtained from fits to g_2(Q,t) through the eq. 3, (see materials and methods).

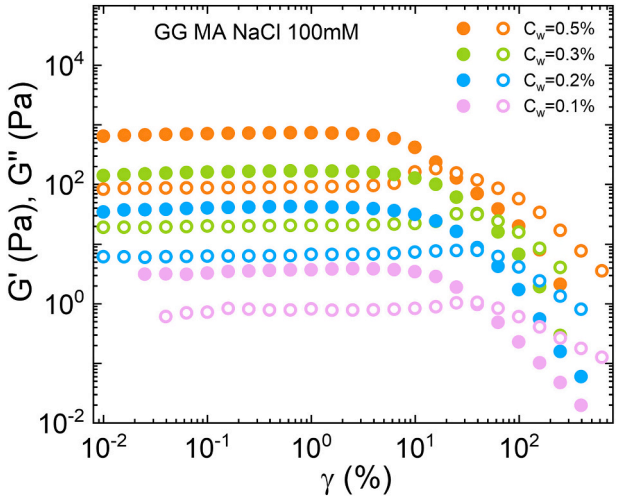

Fig. 14. Storage G′ (closed circles) and loss G″ (open circles) moduli as a function of shear strain γ, at f = 1 Hz, T = 25 °C and C_{NaCl} = 100 mM for GGMA microgels at different concentrations.

grounded in rheological methods, consistently produces stable and highly reproducible microgels.

We provided rheological evidence of the complex two-step aggregation mechanism of GG, highlighted by the presence of a double-yielding behaviour in the flow curves. For hydrogels, this phenomenon was observed at low GG concentrations in the presence of divalent ions, which provide enough rigidity to the gel. Conversely, double yielding was not found in the presence of monovalent salts.

For microgels, we observed a double yielding in the presence of monovalent ions, suggesting that the shear-induced preparation stabilizes the micro-aggregates enhancing their resistant to fracture.

Lastly, our study identifies an optimal rheological window for the storage modulus, which gellan-based systems must satisfy to be efficient in cleaning paper artworks. For hydrogels, this ensures the formation of a rigid gel that does not leave residues on the paper sheet even after one hour of application. For microgels, the low values of the measured stress are less critical since they do not need the application of a weight for cleaning, but involve a removal step using water. These findings are highly relevant not only for paper restoration but also for broader applications, including the treatment of substrates such as canvas and wood, thereby opening new possibilities in art restoration and other fields.

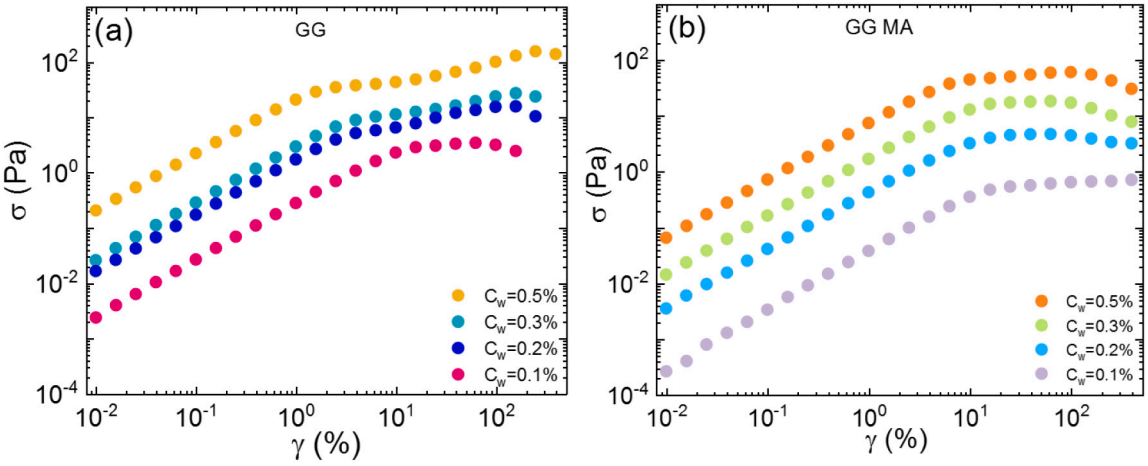

Fig. 15. Shear stress σ as a function of shear strain γ, at f = 1 Hz, T = 25 °C and C_{NaCl} = 100 mM for (a) pure GG and for (b) GGMA microgels at different concentrations with fixed C_{NaCl} = 100 mM.

CRediT authorship contribution statement

Silvia Franco: Writing – review & editing, Writing – original draft, Visualization, Validation, Methodology, Investigation, Formal analysis, Data curation, Conceptualization. **Leonardo Severini:** Writing – review & editing, Visualization, Validation, Investigation, Data curation. **Elena Buratti:** Visualization. **Letizia Tavagnacco:** Visualization. **Simona Sennato:** Writing – review & editing, Visualization. **Laura Micheli:** Visualization. **Mauro Missori:** Writing – review & editing, Visualization, Validation. **Barbara Ruzicka:** Writing – review & editing, Visualization, Validation, Supervision, Formal analysis, Data curation. **Claudia Mazzuca:** Writing - original draft, Writing – review & editing, Visualization, Validation, Supervision, Investigation. **Emanuela Zaccarelli:** Writing - original draft, Writing – review & editing, Visualization, Validation, Supervision, Investigation, Funding acquisition, Conceptualization. **Roberta Angelini:** Writing – review & editing, Writing – original draft, Visualization, Validation, Supervision, Methodology, Investigation, Funding acquisition, Formal analysis, Data curation, Conceptualization.

Declaration of competing interest

The authors declare that they have no known competing financial interests or personal relationships that could have appeared to influence the work reported in this paper.

Acknowledgements

We acknowledge financial support from Regione Lazio through L.R. 13/08 Progetto Gruppo di Ricerca MICROARTE n. prot. A0375-2020-36515 and from ERC POC project MICROTECH (grant agreement no.101066434). RA acknowledges financial support under the National Recovery and Resilience Plan (NRRP), Mission 4, Component 2, Investment 1.1, Call for tender No. 104 published on 2.2.2022 by the Italian Ministry of University and Research (MUR), funded by the European Union – NextGenerationEU – Project PRIN 2022ZA77J2 ICARUS – CUP B53D23009010006. SF activity has been funded by the European Union – Next Generation EU under the Italian Ministry of University and Research (MUR) project ECS00000024 “Ecosistemi dell’Innovazione” – Rome Technopole, public call n. 3277, PNRR – Mission 4, Component 2, Investment 1.5.

Appendix A. Supplementary data

Supplementary data to this article can be found online at https://doi.org/10.1016/j.carbpol.2025.123329.

Data availability

Data for this article is available via zenodo at https://doi.10.5281/zenodo.14779923.

References

Ahuja, A., Potanin, A., & Joshi, Y. M. (2020). Two step yielding in soft materials. *Advances in Colloid and Interface Science, 282*, Article 102179.
Banerjee, S., & Bhattacharya, S. (2012). Food gels: Gelling process and new applications. *Critical Reviews in Food Science and Nutrition, 52*(4), 334–346.
Caggioni, M., Spicer, P. T., Blair, D. L., Lindberg, S. E., & Weitz, D. (2007). Rheology and microrheology of a microstructured fluid: The gellan gum case. *Journal of Rheology, 51*(5), 851–865.
Cai, Z., Guo, Y., Ma, A., & Zhang, H. (2024). Nmr analysis of the side-group substituents in welan gum in comparison to gellan gum. *International Journal of Biological Macromolecules, 254*, Article 127847.
Calero, N., Alfaro, M., Lluch, M., Berjano, M., & Munoz, J. (2010). Rheological behaviour and structure of a commercial esterquat surfactant aqueous system. *Chemical Engineering & Technology: Industrial Chemistry-Plant Equipment-Process Engineering-Biotechnology, 33*(3), 481–488.
Chandrasekaran, R., Millane, R. P., Arnott, S., & Atkins, E. D. (1988). The crystal structure of gellan. *Carbohydrate Research, 175*(1), 1–15.
Clark, A. H. (1992). Gels and gelling. *Physical chemistry of foods, 7*, 263–305.
Compaan, A. M., Song, K., & Huang, Y. (2019). Gellan fluid gel as a versatile support bath material for fluid extrusion bioprinting. *ACS Applied Materials & Interfaces, 11*(6), 5714–5726.
Corsaro, C., Mallamace, D., Vasi, S., Pietronero, L., Mallamace, F., & Missori, M. (2016). The role of water in the degradation process of paper using 1 h hr-mas nmr spectroscopy. *Physical Chemistry Chemical Physics, 18*(48), 33335–33343.
Dai, L., Liu, X., Liu, Y., & Tong, Z. (2008). Concentration dependence of critical exponents for gelation in gellan gum aqueous solutions upon cooling. *European Polymer Journal, 44*(12), 4012–4019.
Dai, L., Liu, X., & Tong, Z. (2010). Critical behaviour at sol–gel transition in gellan gum aqueous solutions with kcl and cacl2 of different concentrations. *Carbohydrate Polymers, 81*(2), 207–212.
D’Arrigo, G., Navarro, G., Di Meo, C., Matricardi, P., & Torchilin, V. (2014). Gellan gum nanohydrogel containing anti-inflammatory and anti-cancer drugs: A multi-drug delivery system for a combination therapy in cancer treatment. *European Journal of Pharmaceutics and Biopharmaceutics, 87*(1), 208–216.
Di Napoli, B., Franco, S., Severini, L., Tumiati, M., Buratti, E., Titubante, M., , … Ruzicka, B., et al. (2020). Gellan gum microgels as effective agents for a rapid cleaning of paper. *ACS Applied Polymer Materials, 2*(7), 2791–2801.
Diener, M., Adamcik, J., Bergfreund, J., Catalini, S., Fischer, P., & Mezzenga, R. (2020). Rigid, fibrillar quaternary structures induced by divalent ions in a carboxylated linear polysaccharide. *ACS Macro Letters, 9*(1), 115–121.
Diener, M., Adamcik, J., Sánchez-Ferrer, A., Jaedig, F., Schefer, L., & Mezzenga, R. (2019). Primary, secondary, tertiary and quaternary structure levels in linear polysaccharides: From random coil, to single helix to supramolecular assembly. *Biomacromolecules, 20*(4), 1731–1739.
D’Oria, G., Zeng, X., Limbach, H. J., Hartmann, C., Ahrné, L., & Gunes, D. Z. (2024). Effect of stirring speed on low acyl gellan gum fluid gels-rheology, particle morphology and physical ageing. *Food Hydrocolloids, 149*, Article 109614.
Fernandez-Nieves, A., Wyss, H., Mattsson, J., & Weitz, D. A. (2011). *Microgel suspensions: Fundamentals and applications*. John Wiley & Sons.
Gajbhiye, S., Dhoble, S., & Tobin, D. (2024). Natural gum (xanthan, gellan, arabic, guar, ghatti gum, etc.)-based bio-scaffold and their application in tissue engineering. In *Natural product inspired scaffolds: Applications in tissue engineering* (pp. 61–91). Springer.
García, M. C., Alfaro, M. C., Calero, N., & Muñoz, J. (2011). Influence of gellan gum concentration on the dynamic viscoelasticity and transient flow of fluid gels. *Biochemical Engineering Journal, 55*(2), 73–81.
García, M. C., Alfaro, M. C., & Muñoz, J. (2016). Rheology of sheared gels based on low acyl-gellan gum. *Food Science and Technology International, 22*(4), 325–332.
Grasdalen, H., & Smidsrød, O. (1987). Gelation of gellan gum. *Carbohydrate Polymers, 7*(5), 371–393.
Grinberg, V. Y., Burova, T. V., Grinberg, N. V., Mashkevich, A. Y., Plashchina, I. G., Usov, A. I., … Cesàro, A. (2003). Thermodynamics of the double helix-coil equilibrium in tetramethylammonium gellan: High-sensitivity differential scanning calorimetry data. *Macromolecular Bioscience, 3*(3–4), 169–178.
Iannuccelli, S., & Sotgiu, S. (2010). Wet treatments of works of art on paper with rigid gellan gels. *The book and paper group annual, 29*(2010), 25–39.
Khaksar-Baghan, N., Koochakzaei, A., & Hamzavi, Y. (2024). An overview of gel-based cleaning approaches for art conservation. *Heritage Science, 18*(48).
Kohlrausch, R. (1854). Thermoresponsive poly-(N-isopropylmethacrylamide) microgels: Tailoring particle size by interfacial tension control. *Pogg. Ann. Phys. Chem., 91*, 179–214.
Matricardi, P., Cencetti, C., Ria, R., Alhaique, F., & Coviello, T. (2009). Preparation and characterization of novel gellan gum hydrogels suitable for modified drug release. *Molecules, 14*(9), 3376–3391.
Mazzuca, C., Micheli, L., Carbone, M., Basoli, F., Cervelli, E., Iannuccelli, S., … Palleschi, A. (2014). Gellan hydrogel as a powerful tool in paper cleaning process: A detailed study. *Journal of Colloid and Interface Science, 416*, 205–211.
Mazzuca, C., Micheli, L., Lettieri, R., Cervelli, E., Coviello, T., Cencetti, C., Sotgiu, S., Iannuccelli, S., Palleschi, G., & Palleschi, A. (2016). How to tune a paper cleaning process by means of modified gellan hydrogels. *Microchemical Journal, 126*, 359–367.
Micheli, L., Mazzuca, C., Palleschi, A., & Palleschi, G. (2016). Development of a diagnostic and cleaning tool for paper artworks: A case of study. *Microchemical Journal, 126*, 32–41.
Milivojevic, M., Pajic-Lijakovic, I., Bugarski, B., Nayak, A. K., & Hasnain, M. S. (2019). Gellan gum in drug delivery applications. *Natural polysaccharides in drug delivery and biomedical applications*, 145–186.
Miyoshi, E., & Nishinari, K. (1999a). Rheological and thermal properties near the sol-gel transition of gellan gum aqueous solutions. *Progress in Colloid and Polymer Science, 114*, 68–82.
Miyoshi, E., & Nishinari, K. (1999b). Non-newtonian flow behaviour of gellan gum aqueous solutions. *Colloid and Polymer Science, 277*, 727–734.
Miyoshi, E., Takaya, T., & Nishinari, K. (1996). Rheological and thermal studies of gel-sol transition in gellan gum aqueous solutions. *Carbohydrate Polymers, 30*(2–3), 109–119.
Morris, E. R., Nishinari, K., & Rinaudo, M. (2012). Gelation of gellan–A review. *Food Hydrocolloids, 28*(2), 373–411.
Musazzi, U. M., Cencetti, C., Franzé, S., Zoratto, N., Di Meo, C., Procacci, P., … Cilurzo, F. (2018). Gellan nanohydrogels: Novel nanodelivery systems for cutaneous administration of piroxicam. *Molecular Pharmaceutics, 15*(3), 1028–1036.

Nagpal, S., Dubey, S. K., Rapalli, V. K., & Singhvi, G. (2019). Pharmaceutical applications of gellan gum. In *Natural polymers for pharmaceutical applications* (pp. 87–109). Apple Academic Press.

Nickerson, M., Paulson, A., & Speers, R. (2003). Rheological properties of gellan solutions: Effect of calcium ions and temperature on pre-gel formation. *Food Hydrocolloids, 17*(5), 577–583.

Oh, J. K., Drumright, R., Siegwart, D. J., & Matyjaszewski, K. (2008). The development of microgels/nanogels for drug delivery applications. *Progress in Polymer Science, 33*(4), 448–477.

Oliveira, J. T., Martins, L., Picciochi, R., Malafaya, P., Sousa, R., Neves, N., … Reis, R. (2010). Gellan gum: A new biomaterial for cartilage tissue engineering applications. *Journal of Biomedical Materials Research Part A: An Official Journal of The Society for Biomaterials, The Japanese Society for Biomaterials, and The Australian Society for Biomaterials and the Korean Society for Biomaterials, 93*(3), 852–863.

Paulsson, M., Hägerström, H., & Edsman, K. (1999). Rheological studies of the gelation of deacetylated gellan gum (gelrite) in physiological conditions. *European Journal of Pharmaceutical Sciences, 9*(1), 99–105.

Pérez-Campos, S. J., Chavarría-Hernández, N., Tecante, A., Ramírez-Gilly, M., & Rodríguez-Hernández, A. I. (2012). Gelation and microstructure of dilute gellan solutions with calcium ions. *Food Hydrocolloids, 28*(2), 291–300.

Picone, C. S. F., & Cunha, R. L. (2011). Influence of ph on formation and properties of gellan gels. *Carbohydrate Polymers, 84*(1), 662–668.

Prajapati, V. D., Jani, G. K., Zala, B. S., & Khutliwala, T. A. (2013). An insight into the emerging exopolysaccharide gellan gum as a novel polymer. *Carbohydrate Polymers, 93*(2), 670–678.

Puoti, F., Jervis, A. V., Ciabattoni, R., Cossa, E., Di Giovanni, A., Giuliani, M. R., & Iodele, M. (2017). *Evaluation of leather cleaning with a rigid hidrogel of gellan gum on two composite amharic shields from the Museo Nazionale Preistorico Etnografico" Luigi Pigorini"*. Rome: Archetype Publications.

Rodríguez-Hernández, A., Durand, S., Garnier, C., Tecante, A., & Doublier, J. L. (2003). Rheology-structure properties of gellan systems: Evidence of network formation at low gellan concentrations. *Food Hydrocolloids, 17*(5), 621–628.

Sabadini, R. C., Martins, V. C., & Pawlicka, A. (2015). Synthesis and characterization of gellan gum: Chitosan biohydrogels for soil humidity control and fertilizer release. *Cellulose, 22*, 2045–2054.

Safronov, A. P., Tyukova, I. S., & Kurlyandskaya, G. V. (2018). Coil-to-helix transition of gellan in dilute solutions is a two-step process. *Food Hydrocolloids, 74*, 108–114.

Saha, D., & Bhattacharya, S. (2010). Characteristics of gellan gum based food gels. *Journal of Texture Studies, 41*(4), 459–471.

Severini, L., Franco, S., Celi, E., Sennato, S., Paialunga, E., Tavagnacco, L., Micheli, L., Angelini, R., Zaccarelli, E., & Mazzuca, C. (2025). Methacrylated gellan gum microgels: A further step in the gel-based cleaning system. *Journal of Cultural Heritage, 71*, 97–105.

Severini, L., Tavagnacco, L., Angelini, R., Franco, S., Bertoldo, M., Calosi, M., , … Ruzicka, B., et al. (2023). Methacrylated gellan gum hydrogel: A smart tool to face complex problems in the cleaning of paper materials. *Cellulose, 30*(16), 10469–10485.

Sworn, G., & Kasapis, S. (1998). Effect of conformation and molecular weight of co-solute on the mechanical properties of gellan gum gels. *Food Hydrocolloids, 12*(3), 283–290.

Sworn, G., Sanderson, G., & Gibson, W. (1995). Gellan gum fluid gels. *Food Hydrocolloids, 9*(4), 265–271.

Tako, M., Teruya, T., Tamaki, Y., & Konishi, T. (2009). Molecular origin for rheological characteristics of native gellan gum. *Colloid and Polymer Science, 287*, 1445–1454.

Tang, J., Tung, M., & Zeng, Y. (1997). Gelling properties of gellan solutions containing monovalent and divalent cations. *Journal of Food Science, 62*(4), 688–712.

Tavagnacco, L., Chiessi, E., Severini, L., Franco, S., Buratti, E., Capocefalo, A., Brasili, F., Mosca Conte, A., Missori, M., Angelini, R., et al. (2023). Molecular origin of the two-step mechanism of gellan aggregation. *Science Advances, 9*(10), Article eadg4392.

Williams, D. C. W. G. (1970). Non-symmetrical dielectric relaxation behaviour arising from a simple empirical decay function. *Journal of the Chemical Society, Faraday Transactions, 66*, 80–85.

Winter, H. H., & Chambon, F. (1986). Analysis of linear viscoelasticity of a crosslinking polymer at the gel point. *Journal of Rheology, 30*(2), 367–382.

Yang, X., Kimura, M., Zhao, Q., Ryo, K., Descallar, F. B. A., & Matsukawa, S. (2024). Gelation of gellan induced by trivalent cations and coexisting trivalent with monovalent cations studied by rheological and dsc measurements. *Carbohydrate Polymers, 122485*.